Journal of Molecular Graphics and Modelling 57 (2015) 20–26

Contents lists available at ScienceDirect

Journal of Molecular Graphics and Modelling

journal homepage: www.elsevier.com/locate/JMGM

Dissipative particle dynamics study on self-assembled platycodin structures: The potential biocarriers for drug delivery

Xingxing Dai[a,b,1], Haiou Ding[c,1], Qianqian Yin[d], Guang Wan[d], Xinyuan Shi[a,b,*], Yanjiang Qiao[a,b,*]

[a] Beijing University of Chinese Medicine, Beijing 100102, China
[b] Key Laboratory of TCM-information Engineer of State Administration of TCM, Beijing 100102, China
[c] Civil Aviation General Hospital, Beijing 100123, China
[d] School of Traditional Chinese Medicine, Capital Medical University, Beijing 100069, China

ARTICLE INFO

Article history:
Accepted 6 January 2015
Available online 15 January 2015

Keywords:
Biosurfactant
Platycodin
Dissipative particle dynamics
Self-assembly
Solubilization
Biocarrier

ABSTRACT

Platycodin, as a kind of plant based biosurfactants, are saponins which derived from the root of *Platycodon grandiflorum* A. DC. It has been confirmed that platycodin have the potential to enhance the solubility of hydrophobic drugs and function as the drug carrier, which depends on their micellization over critical micelle concentration (CMC) in aqueous solutions. With the purpose of investigating the effects of influencing factors on the micellization behavior of platycodin and obtaining the phase behavior details at a mesoscopic level, dissipative particle dynamics (DPD) simulations method has been adopted in this study. The simulations reveal that a rich variety of aggregates morphologies will appear with changes of structure or the concentration of saponins, including spherical, ellipse and oblate micelles and vesicles, multilamellar vesicles (MLVs), multicompartment vesicles (MCMs), tubular and necklace-like micelle. They can be formed spontaneously from a randomly generated initial state and the result has been represented in the phase diagrams. Furthermore, deeper explorations have been done on the concentration-dependent structure variation of spherical vesicles as well as the formation mechanism of MLVs. This work provides insight into the solubilization system formed by platycodin, and may serve as guidance for further development and application in pharmaceutical field of platycodin and other saponins.

1. Introduction

Saponin is one of the most commonly known plant based biosurfactants. Many of them have the ability to promote the solubility of insoluble drugs besides notable pharmacological activity [1–3], and thus have been proposed as safe and effective adjuvant to enhance the absorption of pharmacologically active components through solubilization in one compound [4,5]. Therefore, an increasing demand for natural products with both surfactant properties (such as emulsifying and solubilizing properties) and biological activities (including anticancer and anti-cholesterol effects) has promised saponins a bright future in successful expansion of commercial applications in the food, cosmetics, and pharmaceutical fields [6].

Platycodon grandiflorum A. DC (Campanulaceae) is a well-known traditional Chinese medicine used as an expectorant for pulmonary diseases and a remedy for respiratory disorders. Its main bioactive substance is platycodin, a kind of pentacyclic triterpene saponins which are comprised of a triterpene aglycone and two sugar chains: one chain links at C-3 of the triterpene aglycone part, the other links at C-28 [7]. This special triblock copolymer-like structure will lead to the self-assembly of saponins above the critical micelle concentration (CMC) in aqueous solutions. Simultaneously, some hydrophobic constituents could be enclosed in [8]. It may explain how these saponins can work as solubilizer in traditional Chinese medicine recipes and present their potential in functioning as biocarrier. It has been reported that sugar chains of platycodin have significant effects on their surfactivity [7], however, whether or how does this moiety influence the performance of platycodin working as solubilizer or biocarrier have not been mentioned.

According to the architecture and concentration of copolymer, amphiphilic block copolymers can self-assemble into various morphologies, such as spheres, rods, vesicles, tubules, multilamellar

* Corresponding authors at: Beijing University of Chinese Medicine, 100102 China. Tel.: +86 10 84738621; fax: +86 10 84738661.
E-mail addresses: shixinyuan01@163.com (X. Shi), yjqiao@263.net (Y. Qiao).
[1] These authors contributed equally to this work.

http://dx.doi.org/10.1016/j.jmgm.2015.01.002
1093-3263/

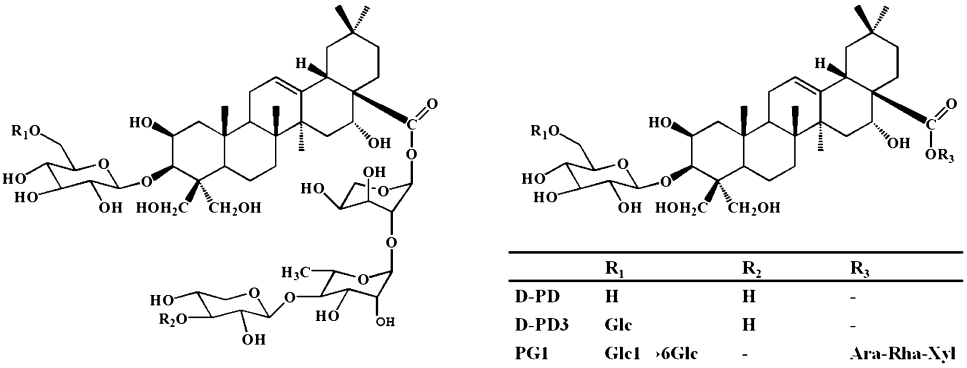

	R_1	R_2	R_3
D-PD	H	H	-
D-PD3	Glc	H	-
PG1	Glc1 ›6Glc	-	Ara-Rha-Xyl
PD	H	Api	-
PD3	Glc	Api	-
PE	Glc1 ›6Glc	Api	-

Fig. 1. Chemical structures of 6 platycodins.

vesicles (MLVs) and multicompartment vesicles (MCMs). And these morphologies have significant impacts on their solubilization and drug loading performances [9–13]. So do the saponins. However, there are few studies paying attention to the influences of structure on the morphologies formed by saponins either to the underlying forming mechanisms of them.

Up to now, the self-assembly of saponins have been investigated by numerous experimental techniques, including transmission electron microscopy (TEM), dynamic light scattering (DLS) and so on [8,14]. These experimental results show that saponins can self-assemble to various morphologies, which are influenced by their molecular structure, concentration and the solution environment [15]. However, due to the limitations in both time and spatial scale, it is difficult to observe the details and visualize the evolution process of these morphologies directly at a molecular level by experimental techniques. With the purpose of clarifying the structure-function relationship, dissipative particle dynamics (DPD) method was employed. DPD is an effective mesoscopic simulation technique and has been extensively employed in the studies of self-assembly of amphiphile [16–21]. Recently, our team has adopted this method in the research of saponins self-assembly and solubilization and got a sequence of interesting findings [8,14,22]. In this study, the self-assembly of saponins with same hydrophobic aglycon while different sugar chains in terms of the number was studied to make a more comprehensive understanding.

What is more, further explorations were made on those important micelles, such as vesicles and MLVs, which have been taken as the ideal carriers in the food, cosmetics, and pharmaceutical fields. This work is organized as follow. In Section 2, we briefly outline the DPD method, then, we describe model and simulation parameters in detail. Section 3 contains result and discussion, including three aspects: comparisons on the morphologies evolving with concentration of different saponins; concentration-dependent variation of vesicles formed by platycodin D (PD); forming process analysis of MLVs self-assembled by deapio-platycodin D (D-PD). Our final conclusions are given in Section 4.

2. Simulation method

2.1. Description of DPD method

The DPD method has been explained extensively and in details elsewhere [23], so we only give a brief description here. DPD employed Newton's equation of motion to govern the time evolution of a many-body system through numerical integration. Hence, at every time step, the set of positions and velocities ($\mathbf{r}_i$,$\mathbf{v}_i$) follows from the positions and velocities at earlier time.

$$\frac{d\mathbf{r}_i}{dt} = \mathbf{v}_i, \quad m_i \frac{dv_i}{dt} = \mathbf{f}_i \tag{1}$$

For simplicity, the masses of all particles are set to 1 DPD unit [24], $\mathbf{r}_i$,$\mathbf{v}_i$, m_i and $\mathbf{f}_i$ denote the position vector, velocity, mass, and total force acting on particle i, respectively.

The sum $\mathbf{f}_i$ between each pair of beads contains three parts: a harmonic conservative interaction force ($\mathbf{F}_{ij}^C$), which is soft repulsion acting along the line of centers; a dissipative force ($\mathbf{F}_{ij}^D$), which represents the viscous drag between moving beads; and a random force ($\mathbf{F}_{ij}^R$), which maintains energy input into the system in opposition to the dissipation. The drag force ($\mathbf{F}_{ij}^D$) and the random force ($\mathbf{F}_{ij}^R$) act as heat sink and source respectively, so their combined effect is a thermostat. All forces are short-range with a fixed cut-off radius r_c, which is usually chosen as the reduced unit of length $r_c = 1$. They are given as follows:

$$\mathbf{f}_i = \sum\nolimits_{j \neq i} (\mathbf{F}_{ij}^C + \mathbf{F}_{ij}^D + \mathbf{F}_{ij}^R) \tag{2}$$

$$\mathbf{F}_{ij}^C = \begin{cases} a_{ij}(1 - r_{ij})\mathbf{r}_{ij} & (r_{ij} < 1) \\ 0 & (r_{ij} \geq 1) \end{cases} \tag{3}$$

$$\mathbf{F}_{ij}^D == -\gamma w^D(r_{ij})(\hat{\mathbf{r}}_{ij} \cdot \mathbf{v}_{ij})\hat{\mathbf{r}}_{ij} \tag{4}$$

$$\mathbf{F}_{ij}^R == \sigma w^R(r_{ij})\xi_{ij}\frac{1}{\sqrt{\Delta t}}\hat{\mathbf{r}}_{ij} \tag{5}$$

Here, a_{ij} is a maximum repulsion between particle i and particle j; $\mathbf{r}_{ij} = \mathbf{r}_i - \mathbf{r}_j$, $r_{ij} = |\mathbf{r}_{ij}|$, $\hat{\mathbf{r}}_{ij} = \mathbf{r}_{ij}/|\mathbf{r}_{ij}|$; γ is the dissipation strength; σ is the noise strength; w^D and w^R are r-dependent weight functions vanishing for $r > 1$; ξ_{ij} is a random number with zero mean and unit variance, and Δt is the time step of the simulation.

2.2. Model, parameters and simulation conditions

The platycodins that have been taken into consideration in this study include deapio-platycodin D (D-PD), deapio-platycodin D3 (D-PD3), platycodin G1 (PG1), platycodin D (PD), platycodin D3 (PD3), and platycodin E (PE). Their chemical structures are shown in Fig. 1. These saponins contain same hydrophobic pentacyclic triterpenoid aglycone, but different number of hydrophilic sugars in two sugar chains: a links at C-3 and b links at C-28 of the triterpene aglycone part. Taking the ring-like structure as a unit, the molecular structure of platycodin is divided into three types of particles

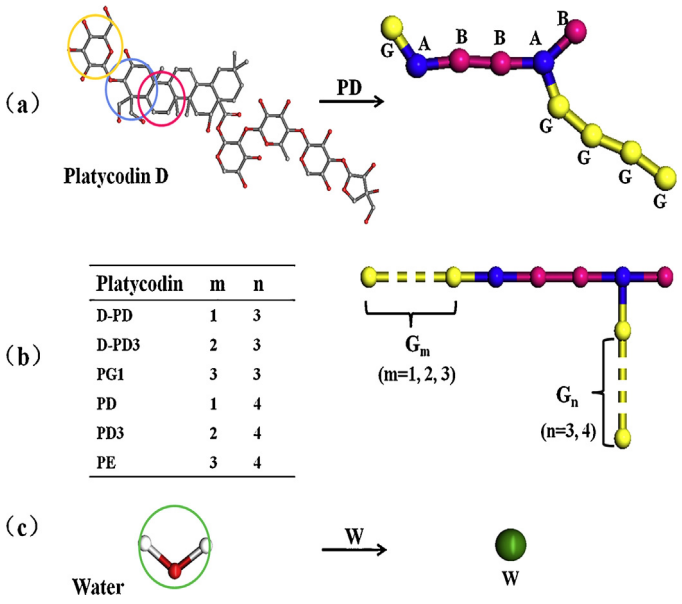

Fig. 2. Chemical structures and coarse-grained models of platycodin and water. (a) Coarse grained details of platycodin D; (b) the platycodin; (c) water.

according to the polarity of atoms group they present. The ring-like structures in the aglycone linked with sugar chain are taken as bead A, and the others in the aglycone are named as bead B. Because there is no significant difference between different sugars in solubility parameter, all kinds of sugar molecules are marked as one kind of bead G (representing glucose) to focus the research target on the influence of the number of sugar and to expand the applicability of the study at the same time (see Section S1 in supplemental material). The order of the polarity is G > A > B. The solvent water particles are represented by bead W [23]. Simple coarse-grained models of the components used in this study are shown in Fig. 2.

For calculating conservation force, Groot and Warren [23,24] have made a link between the repulsive parameter (a_{ij}) and Flory–Huggins parameters χ_{ij}. To maintain the compressibility of water at room temperature, the repulsion parameter has to be calculated based on Eq. (6)

$$a_{ij}\rho = 75k_BT \tag{6}$$

In this equation k_B is the Boltzmann constant and T is the system temperature. The particle density $\rho = 3$ and $k_BT = 1$ have been used in this simulation. The values of repulsion parameters between different types of particles are related with the Flory–Huggins parameters χ_{ij} linearly, shown as:

$$a_{ij} = a_{ii} + 3.5\chi_{ij} \tag{7}$$

The value of χ_{ij} can be obtained from Eq. (8)

$$\chi_{ij} = \frac{(\delta_i - \delta_j)^2 V}{RT} \tag{8}$$

Here, V is the arithmetic average of molar volumes of beads i and j, δ_i and δ_j are the solubility parameters, which depend on the chemical nature of species and can be obtained through the molecular dynamics (MD) simulation. In this study, solubility parameters are calculated using the Amorphous Cell module in Materials Studio 5.5 (Accelrys Inc., supported by CHEMCLOUDCOMPUTING) with the COMPASS force field. The repulsion parameters a_{ij} used in DPD are shown in Table 1.

Considering the simulation quality and computation efficiency, the three-dimensional periodic box of $20 \times 20 \times 20\, r_c^3$ (which was proved enough to avoid the finite size in our pre-test (see Fig. S1 in supplemental material)) and the integration time step of $0.05t_c$ are taken (r_c and t_c are DPD length and time unit respectively). All the simulations start from a randomly dispersed condition, and the total simulation involved 50,000 steps, which is long enough for the simulation system to reach equilibrium (see Fig. S2 in supplemental material). The spring constant is fixed at 4.0, which will ensure reasonable results in our study system [25].

Table 1
Repulsion parameters a_{ij} used in DPD simulations.

	G	A	B	W
G	25.00			
A	32.92	25.0		
B	57.94	39.93	25.0	
W	42.16	72.24	99.07	25.0

The average volume of beads is 148 Å^3 here, and the number density is ($\rho r_c^3 = 3$). Thus, a natural length scale in the simulations can be obtained: $r_c = \sqrt[3]{3 \times 148} = 7.63$ Å . The time unit $t_c = r_c\sqrt{m_c/k_BT} = 0.0054$ ns where $m_c = 130$ amu is the average mass of beads [26,27]. Although the time and length of our simulations could not quantitatively relate to the physical systems, it can still provide a great deal of useful qualitative information, which may promote the understanding of the solubilization mechanism of saponin.

3. Results and discussion

3.1. Comparison on morphologies evolving with concentration

In this section, we perform simulations to study the concentration-dependent morphologies of the six saponins in aqueous solution with concentration ranged from 1.0 vol% to 18.0 vol%. These saponins have the same hydrophobic portions, so the differences in their phase separation behaviors and micelle structures in the equilibrium state will be simply contributed by their hydrophilic part, the sugar chains, which are comprised of same bead G here. For comparison, the simulation results have been presented in morphology diagrams in terms of the saponins' concentration (C_P) and the ratio of the solvophilic bead G (R_G). All the spontaneous aggregation processes start from a randomly dispersed system.

According to the difference in R_G, the transformations of aggregation morphologies along with changing concentration of the six saponins present different rules. D-PD, D-PD3 and PD, whose R_G is less than or equal to 0.5, at low concentration from 2.0 vol% to 4.0 vol%, formed into spherical micelles (Fig. 3a), ellipse micelles (Fig. 3b) except for D-PD and oblate micelles (Fig. 3c) in sequence. With C_P increasing, both D-PD and PD form into semivesicles (Fig. 3d and e) and spherical vesicles (Fig. 3f). PD, with one more sugar in chain b than D-PD, shows wider concentration span in every phase than D-PD, especially the spherical vesicles phase which lasts from 10.0 vol% to 18.0 vol%. Whereas before the phase of spherical vesicles, D-PD3 forms into the basket-shaped MCMs. After the spherical vesicles phase, the ellipse vesicles (Fig. 3g) and oblate vesicles (Fig. 3h) successively appeared both in D-PD and D-PD3's array. And these morphologies, including spherical vesicles, ellipse vesicles and oblate vesicles of these two saponins almost have the same concentration intervals. D-PD3, also with one more sugar than D-PD in chain A, shows a delay in every concentration point of phase transitions. When C_p increase to 16.0 vol%, D-PD forms into MLVs (Fig. 3i). Among these saponins, only D-PD has this morphology within or even beyond the concentration range investigated here. This finding is similar to what Harris has reported, that surfactant with shorter solvophilic chains favor the formation of MLVS for a given solvophobic chains length [28]. The detailed

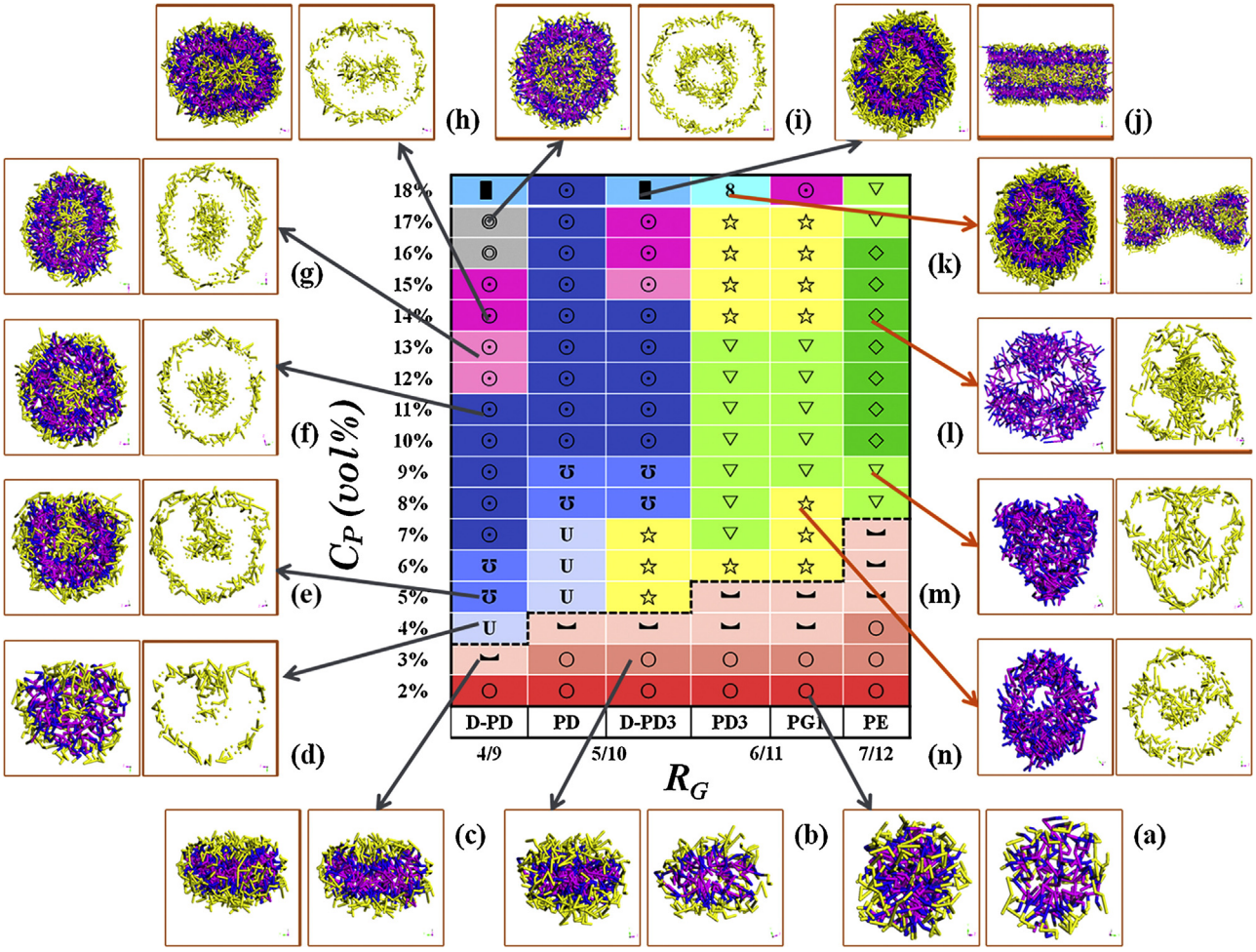

Fig. 3. Morphology diagram of platycodins in aqueous solution in terms of ratio of the solvophilic bead G (R_G) and the saponins' concentration (C_P). The same symbols represent similar morphologies, and the different background colors refer to that there are differences in these similar morphologies. Representative snapshots of the micelle morphologies are shown. The labels in the snapshots correspond to (a) spherical micelles, (b) ellipse micelles, (c) oblate micelles, (d, e) semivesicles, (f) spherical vesicles, (g) ellipse vesicles, (h) oblate vesicles, (i) multilamellar vesicles (MLVs), (j) tubules, (k) necklace-like micelle, (l) basket-shaped MCMs, (m) tee shaped MCMs, (n) tetrahedron shaped MCMs. For clarity, structure of (a), (b) and (c) are shown in overall views and section views; morphologies of (d)–(i) are demonstrated by middle section views and views of middle slice of bead G's skeleton; structures of (j) and (k) are stated by two section views which are perpendicular to and parallel to the axis respectively; structure from (l) to (n) are separately represented by the frame of bead A, B and the profile of bead G. Color scheme in the snapshots: G (yellow), A (blue) and B (roseo). (For interpretation of the references to color in this figure legend, the reader is referred to the web version of this article.)

forming process of MLVs will be shown in Section 3.3. At 18.0 vol%, tubules (Fig. 3j) appeared both for D-PD and D-PD3.

PD3, PG1 and PE, whose R_G is larger than 0.5, also share the spherical micelles – ellipse micelles – oblate micelles stage at low concentration. While beyond the concentration of oblate micelles, they represent a novel morphology map. It is comprised of MCMs with various architectures, such as basket-shape (two holes distributioned amesiality), tee shape (three holes with a symmetrical arrangement) and tetrahedron shape (four holes with a symmetrical arrangement) in terms of the solvophobic profile constructed by bead A and B. These hydrophobic shell are both coated and filled by the hydrophilic bead G. Meanwhile, the inner bead G connect with outer ones through the holes on the hydrophobic shell as showed in Fig. 3l–n. PD3 and PG1 have the same R_G, and their dominant morphologies are basket-shaped and tee shaped MCMs. With C_P increasing, the aggregates change in a "basket-shape-tee shape-basket-shape" order. At 18.0 vol%, necklace-like micelles (Fig. 3k) and oblate vesicles respectively appear for PD3 and PG1. In terms of PE, whose R_G is the biggest, its morphology array is almost occupied by the tetrahedron shaped MCMs from 10.0 vol% to 16.0 vol%, the tee shaped MCMs appear at both sides for 8.0 vol%, 9.0 vol% and 17.0 vol%, 18.0 vol%.

At low concentration, almost all these saponins have the three-step morphology transformation: spherical micelles – ellipse micelles – oblate micelles. Obviously, an increase in R_G will result in the expansion of concentration range of oblate micelles. It is confirmed that an oblate micelles is an important intermediate state to form vesicles, which will minimize the hydrophobic interaction energy on the borders of oblate micelles. When the size of the amphiphiles is not the same, the number of amphiphiles to form a vesicle is different. It is observed that larger amphiphiles show slow dynamics and demands a large number of molecules for vesicle formation [29] which is consistent nicely with our result. With C_P increasing, saponins with smaller R_G prefer the structures like spherical vesicles, ellipse vesicles and oblate vesicles, which possess an intact hydrophobic shell, whereas saponins with larger R_G favor the formation of MCMs, which have the separated hydrophobic part. The more sugars saponin contains the more compartments the formed vesicles have. Here, PD and D-PD3, PD3 and PG1, both groups are comprised of two saponins with the same R_G while different allocation of bead G in the two sugar chains. At low concentration, they have the same behavior. With C_P increasing, however, the differences in their aggregate performance turn up and mainly are reflected in three aspects: the morphologies, the

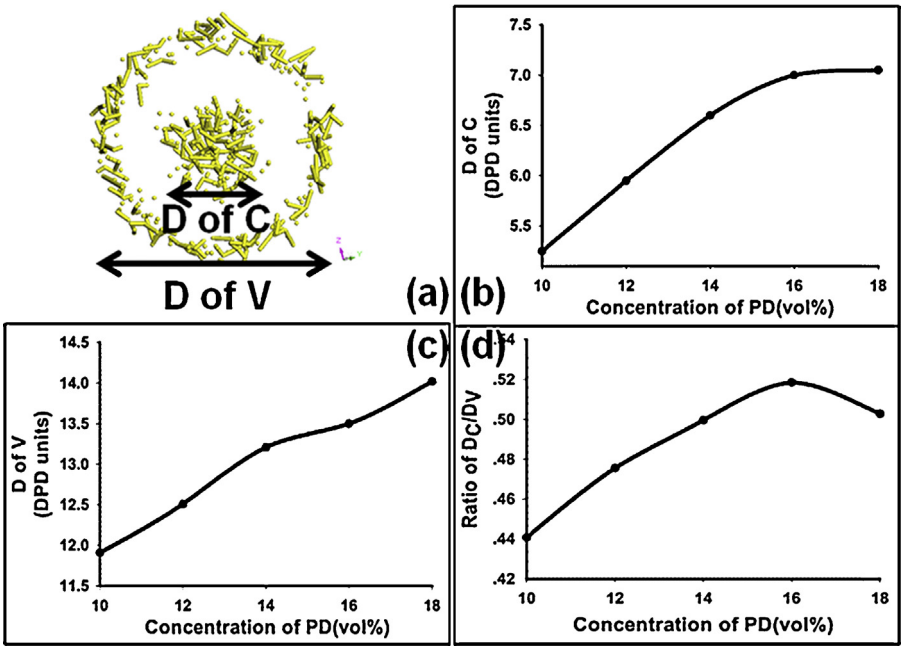

Fig. 4. Concentration-dependent diameters variation of PD vesicles. (a) View of middle slice of bead G's skeleton, (b) diameter of inner hydrophilic core, (c) diameter of vesicle, (d) ratio of diameter of inner hydrophilic core to diameter of vesicle.

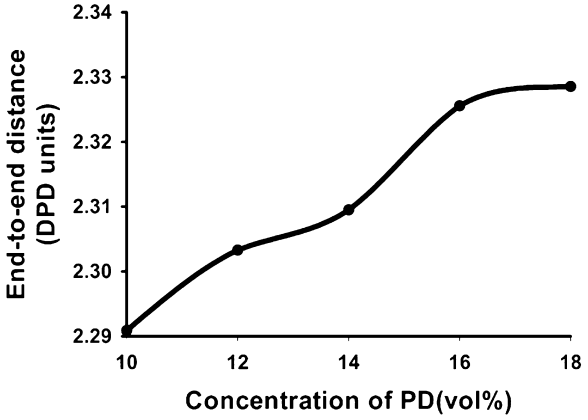

Fig. 5. Concentration-dependent end-to-end distance variation of PD vesicles.

concentration interval of same morphology, and the concentration at which the same morphology formed.

What can be concluded from the simulation results is that both the hydrophobic/hydrophilic ratio and the sugars' allocation in the two sugar chains have large effects on the morphologies of saponins. By changing these factors, morphologies can be tuned. Furthermore, the various structures of micelles identified in this work indicate that saponins can also provide complicated structures and may contribute more choices in drug delivery system.

3.2. Concentration-dependent structural variation of spherical vesicles

In Section 3.1, the structure and concentration-dependent morphology were investigated, a conclusion can be drawn that spherical vesicles are staple morphology of D-PD, D-PD3 and PD at relative higher concentrations. The core-shell-corona structures of these spherical vesicles enable them not only to load hydrophobic drugs but also to carry the hydrosoluble ones. So it is requisite to operate deeper researches on them. Because the vesicles morphology of these saponins share the same variation process with

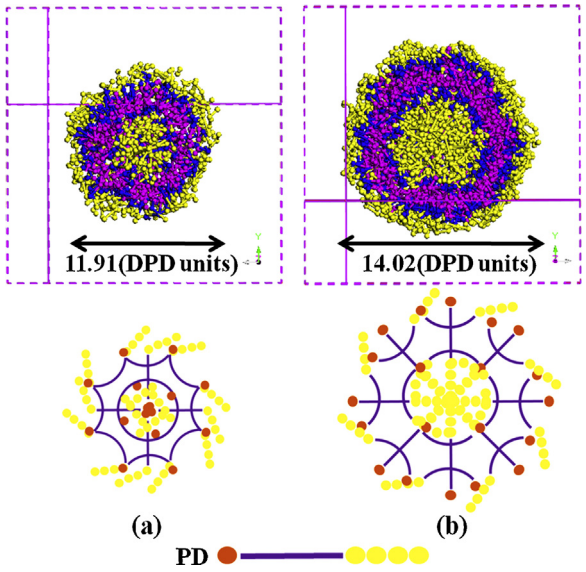

Fig. 6. Section views of PD vesicles and their schematic drawings. (a) 10.0 vol%, (b) 18.0 vol%.

concentration increasing, and PD is dominant in platycodin in terms of its content and pharmacological activity. So, we choose PD as an example to give some further explanations here. With concentration increasing, the diameter of vesicle hydrophilic core gradually increases till 16.0 vol%, and then it changes slightly (Fig. 4b) while the diameter of vesicle rises linearly (Fig. 4c). Fig. 4d shows the change in ratio of diameter of inner hydrophilic core to diameter of vesicle with concentration increasing. From 10.0 vol% to 16.0 vol%, it rises lineally and reaches its max maximum at 16.0 vol%, after that it declines. This indicates that the loading capacity of hydrophilic drugs in vesicles changes with variation of concentration and it has a limitation.

End-to-end distance is a concept derived from polymers which describes the degree of curliness in polymer chain [30], defined as the distance between one end of the polymer chain and the

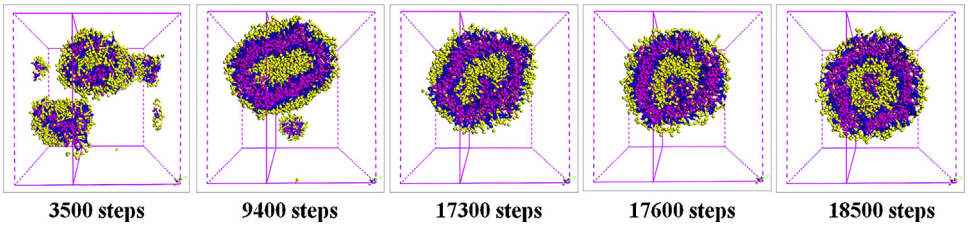

Fig. 7. Snapshots of MLVs forming process.

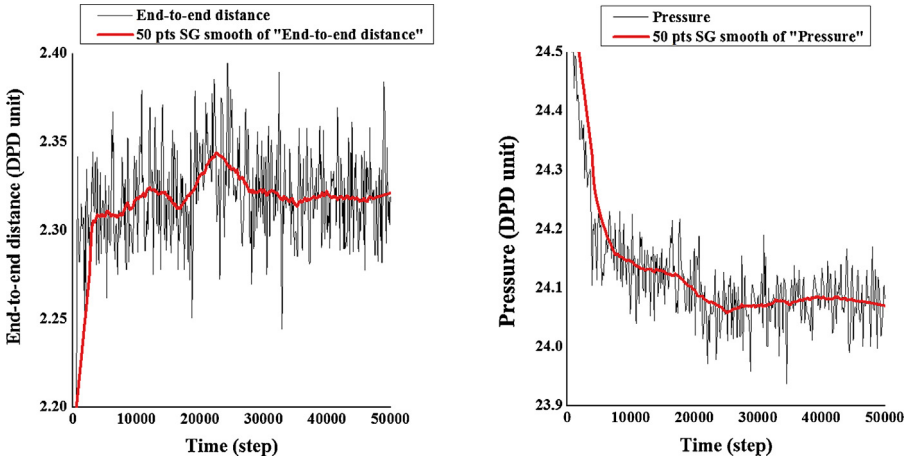

Fig. 8. End-to-end distance and system pressure of MLVs forming process.

other. Here we adopt it to account for the changes of structure of PD molecules in vesicles. As shown in Fig. 5, the end-to-end distance shows a stepwise growth with concentration increasing, and it changes slightly from 16.0 vol% to 18.0 vol%. That indicates the PD molecules become more and more stretched with the increase in concentration until 16.0 vol%. After that, the PD molecules mainly retain their structures at this scale. Further study on the arrangement of PD molecules showed that, PD molecules had three different ways to locate inside the vesicle (Fig. 6). One arrange along the corona, one surround the core, and the other across the shell, leaving its beads G in core or corona. With the rise of concentration, the volume of both vesicles and hydrophilic core area enlarged with the molecules gradually stretched to their extreme length on the concentration from 16.0 vol% to 18.0 vol%. That explained the growth tendency of end-to-end distance. When the concentration is higher than 18.0 vol%, the vesicles enlarged in a one-dimensional radial direction limited by the length of the molecules, and formed ellipsoidal vesicles as shown in Fig. 3.

3.3. *Forming process of multilamellar vesicles*

Multilamellar vesicles show great potential as controlled-release carrier for water-insoluble pharmaceutical and personal care products. Compared to unilamellar vesicles, these structures have a much larger hydrophobic volume for encapsulating hydrophobic agents [29]. In recent years, many researches on the synthesis and characterization of MLVs have been done. Almost all of them are obtained by self-assembly of synthetic surfactants [31–39]; there is no report about the MLVs formed by saponins yet. Due to the limitation in experiment method, the forming process of MLVs has not been observed either. Thus this section will introduce the forming process of D-PD MLVS in purpose of providing some references in the fabrication of MLVs. The process and the corresponding change of end-to-end distance and system pressure are demonstrated in Figs. 7 and 8. The process of spontaneous aggregation starts from a randomly dispersed system. At 3500 time steps, the saponin molecules gather into micelles and semivesicles. With time going on, the aggregates gradually fuse together, at 9400 time steps, there exist only one oblate vesicle and a small spherical micelle in the system. This process results in the enlarged volume of aggregation. Additionally, the saponin molecules become more stretched when the oblate vesicles form. Therefore, the end-to-end distance increases and the system pressure drops down. At 17,300 time steps, the merger happens. Because of the instability of the newly formed morphology, the hydrophobic shell begins to pit and a bud forms in order to reduce the interface energy and recover to a sphere. The bud becomes bigger at 17,600 time steps and then detaches from the shell at 18,500 time steps. In the meantime, the new hydrophobic core forms, and the former hydrophilic core turns to a hydrophilic shell and the MLVs take shape. During the pitting process, the end-to-end distance is decreased because molecules in the pitting direction are compressed. After that, the compressed molecules gradually diffuse and stretch within the MLVs to reach its equilibrium stage. The system pressure also has little changes then.

4. Conclusion

In this work, DPD simulation method is adopted, which can offer valuable microscopic insights and give a preview of phenomena prior to future experimental studies on the aggregation. The simulations show that the structure of sugar chain has great effects on the aggregation morphologies of platycodin. Saponins that have fewer sugars favor the formation of vesicles while the sugar-rich saponins tend to form as MCMs. With the changes of the structure or the concentration of saponins, a rich variety of aggregates would appear, including spherical, ellipse and oblate micelles, vesicles, multilamellar vesicles (MLVs), multicompartment vesicles (MCMs), tubular and necklace-like micelle. To our knowledge, there is little research on the morphologies of saponin aggregates, and

only spherical, wormlike micelles and spherical vesicles have been observed previously [8,40,41].

Vesicles and MLVs have been taken as the ideal carriers in pharmaceutical fields. Deeper explorations have been done on spherical vesicles, which reveals that not only the size and the inner ratio of vesicles will be changed with the growth in concentration. In addition, the arrangement of saponin molecules in vesicles will also adjust correspondingly. Furthermore, the formation mechanism of MLVs has been illustrated, which can be seen as an inside-toward fission process.

With the increasing concern for the natural product, saponins show greater potential in the field of pharmaceutics. Our simulation results enrich the knowledge of the self-assembly morphologies of saponins. It also indicates that saponins have great application potential in solubilization and biocarrier system.

Acknowledgements

This work was financially supported by the National Natural Science Foundation of China (81073058), the National Natural Science Foundation of China (81473364) and the New Century Excellent Talents Program of the Ministry of Education (NCET-12-0803).

Appendix A. Supplementary data

Supplementary data associated with this article can be found, in the online version, at http://dx.doi.org/10.1016/j.jmgm.2015.01.002.

References

[1] O. Tanaka, N. Yata, Promotion of Absorption of Drugs Administered Through the Alimentary System, Wakunaga Yakuhin Kabushiki Kaisha, United States, 1985.
[2] U. Walthelm, K. Dittrich, G. Gelbrich, T. Schopke, Effects of saponins on the water solubility of different model compounds, Planta Med. 67 (2001) 49–54.
[3] S. Tsuzaki, S. Wanezaki, H. Araki, Flavonoid Solubilizion Agent and Method of Solubilizing Flavonoid, Fuji Oil Company, Limited, United States, 2008.
[4] Tsuzaki, S., Wanezaki, S., Araki, H. Flavonoid solubilizion agent and method of solubilizing flavonoid. Google Patents, 2008.
[5] Tanaka, O., Yata, N. Promotion of absorption of drugs administered through the alimentary system. Google Patents, 1985.
[6] O. Guclu-Ustundag, G. Mazza, Saponins: properties, applications and processing, Crit. Rev. Food Sci. Nutr. 47 (2007) 231–258.
[7] H. Sun, L. Chen, J. Wang, K. Wang, J. Zhou, Structure–function relationship of the saponins from the roots of *Platycodon grandiflorum* for hemolytic and adjuvant activity, Int. Immunopharmacol. 11 (2011) 2047–2056.
[8] X. Dai, X. Shi, Y. Wang, Y. Qiao, Solubilization of saikosaponin a by ginsenoside Ro biosurfactant in aqueous solution: mesoscopic simulation, J. Colloid Interface Sci. 384 (2012) 73–80.
[9] S. Pispas, N. Hadjichristidis, I. Potemkin, A. Khokhlov, Effect of architecture on the micellization properties of block copolymers: A(2)B miktoarm stars vs AB diblocks, Macromolecules 33 (2000) 1741–1746.
[10] E. Minatti, R. Borsali, M. Schappacher, A. Deffieux, V. Soldi, T. Narayanan, et al., Effect of cyclization of polystyrene/polyisoprene block copolymers on their micellar morphology, Macromol. Rapid Commun. 23 (2002) 978–982.
[11] G. Riess, Micellization of block copolymers, Prog. Polym. Sci. 28 (2003) 1107–1170.
[12] J. Xu, E.R. Zubarev, Supramolecular assemblies of starlike and V-shaped PB-PEO amphiphiles, Angew. Chem. Int. Ed. 43 (2004) 5491–5496.
[13] G.D. Fu, S.J. Phua, E.T. Kang, K.G. Neoh, Tadpole-shaped amphiphilic block-graft copolymers prepared via consecutive atom transfer radical polymerizations, Macromolecules 38 (2005) 2612–2619.
[14] X. Dai, X. Shi, Q. Yin, H. Ding, Y. Qiao, Multiscale study on the interaction mechanism between ginsenoside biosurfactant and saikosaponin a, J. Colloid Interface Sci. 396 (2013) 165–172.
[15] W. Yuguang, D. Haiou, D. Xingxing, S. Xinyuan, Q. Yanjiang, Development of mesoscopic simulation studies on nonionic block copolymer surfactants, World Sci. Technol. 14 (2012) 1468–1472.
[16] M. Whittle, E. Dickinson, On simulating colloids by dissipative particle dynamics: issues and complications, J. Colloid Interface Sci. 242 (2001) 106–109.
[17] S. Yamamoto, Y. Maruyama, S.-A. Hyodo, Dissipative particle dynamics study of spontaneous vesicle formation of amphiphilic molecules, J. Chem. Phys. 116 (2002) 5842–5849.
[18] Y.M. Lam, G. Goldbeck-Wood, C. Boothroyd, Mesoscale simulation and cryo-TEM of nanoscale drug delivery systems, Mol. Simul. 30 (2004) 239–247.
[19] A. Maiti, J. Wescott, G. Goldbeck-Wood, Mesoscale modelling: recent developments and applications to nanocomposites, drug delivery and precipitation membranes, Int. J. Nanotechnol. 2 (2005) 198–214.
[20] J.-Y. Pang, X. Lue, J. Zhang, S.-L. Yuan, G.-Y. Xu, Mesoscopic simulations on the aggregation behavior of polymeric surfactants in aqueous solutions, Acta Phys. Chim. Sin. 27 (2011) 520–529.
[21] L.S. Zheng, Y.Q. Yang, X.D. Guo, Y. Sun, Y. Qian, L.J. Zhang, Mesoscopic simulations on the aggregation behavior of pH-responsive polymeric micelles for drug delivery, J. Colloid Interface Sci. 363 (2011) 114–121.
[22] X. Dai, X. Shi, H. Ding, Q. Yin, Y. Qiao, Dissipative particle dynamics simulation of Ginsenoside Ro vesicular solubilization systems, J. Comput. Theor. Nanosci. 11 (2014) 2046–2054.
[23] R.D. Groot, P.B. Warren, Dissipative particle dynamics: bridging the gap between atomistic and mesoscopic simulation, J. Chem. Phys. 107 (1997) 4423–4435.
[24] R.D. Groot, T.J. Madden, Dynamic simulation of diblock copolymer microphase separation, J. Chem. Phys. 108 (1998) 8713–8724.
[25] J.G.E.M. Fraaije, B.A.C. van Vlimmeren, N.M. Maurits, M. Postma, O.A. Evers, C. Hoffmann, et al., The dynamic mean-field density functional method and its application to the mesoscopic dynamics of quenched block copolymer melts, J. Chem. Phys. 106 (1997) 4260–4269.
[26] R.D. Groot, K.L. Rabone, Mesoscopic simulation of cell membrane damage, morphology change and rupture by nonionic surfactants, Biophys. J. 81 (2001) 725–736.
[27] G. Scocchi, P. Posocco, M. Fermeglia, S. Pricl, Polymer-clay nanocomposites: a multiscale molecular modeling approach, J. Phys. Chem. B 111 (2007) 2143–2151.
[28] J.K. Harris, G.D. Rose, M.L. Bruening, Spontaneous generation of multilamellar vesicles from ethylene oxide/butylene oxide diblock copolymers, Langmuir 18 (2002) 5337–5342.
[29] E.A. Di Marzio, The ten classes of polymeric phase transitions: their use as models for self-assembly, Prog. Polym. Sci. 24 (1999) 329–377.
[30] F.L. Dong, Y. Li, P. Zhang, Mesoscopic simulation study on the orientation of surfactants adsorbed at the liquid/liquid interface, Chem. Phys. Lett. 399 (2004) 215–219.
[31] J. Juárez, P. Taboada, M.A. Valdez, V. Mosquera, Self-assembly process of different poly(oxystyrene)-poly(oxyethylene) block copolymers: spontaneous formation of vesicular structures and elongated micelles, Langmuir 24 (2008) 7107–7116.
[32] Y. Zhu, H. Yu, J. Zhu, G. Zhao, W. Jiang, X. Yang, Morphological transition of dry vesicles into onion-like multilamellar micelles induced through heating at high temperature, Chem. Phys. Lett. 460 (2008) 257–260.
[33] T. Lu, X. Yao, G.Q. Lu, Y. He, Controlled evolution from multilamellar vesicles to hexagonal mesostructures through the addition of 1,3,5-trimethylbenzene, J. Colloid Interface Sci. 336 (2009) 368–373.
[34] P.D. Petrov, M. Drechsler, A.H.E. Mueller, Self-assembly of asymmetric poly(ethylene oxide)-block-poly (*n*-butyl acrylate) diblock copolymers in aqueous media to unexpected morphologies, J. Phys. Chem. B 113 (2009) 4218–4225.
[35] Y.Y. Chieng, S.B. Chen, Complexation of cationic polyelectrolyte with anionic phospholipid vesicles: concentration, molecular weight and salt effects, J. Colloid Interface Sci. 354 (2011) 226–233.
[36] P. De Maria, A. Fontana, G. Siani, E. D'Aurizio, G. Cerichelli, M. Chiarini, et al., Synthesis and aggregation behaviour of a new sultaine surfactant, Colloids Surf. B: Biointerfaces 87 (2011) 73–78.
[37] H. Gevgilili, D. Kalyon, E. Birinci, M. Malik, L. Goovaerts, R. Bacon, et al., Dynamic assembly of anionic surfactant into highly-ordered vesicles, J. Colloid Interface Sci. 356 (2011) 579–588.
[38] N.V. Salim, Q. Guo, Multiple vesicular morphologies in AB/AC diblock copolymer complexes through hydrogen bonding interactions, J. Phys. Chem. B 115 (2011) 9528–9536.
[39] D. Wang, R. Dong, P. Long, J. Hao, Photo-induced phase transition from multilamellar vesicles to wormlike micelles, Soft Matter 7 (2011) 10713–10719.
[40] S. Mitra, S.R. Dungan, Micellar properties of quillaja saponin. 1. Effects of temperature, salt, and pH on solution properties, J. Agric. Food Chem. 45 (1997) 1587–1595.
[41] M.P.G. Peixoto, J. Treter, P.E. de Resende, N.P. da Silveira, G.G. Ortega, M.J. Lawrence, et al., Wormlike micellar aggregates of saponins from *Ilex paraguariensis* A. St. Hil. (mate): a characterisation by Cryo-TEM, rheology, light scattering and small-angle neutron scattering, J. Pharm. Sci. 100 (2011) 536–546.